

Solvent-in-Salt Electrolytes for Fluoride Ion Batteries

Omar Alshangiti, Giulia Galatolo, Gregory J. Rees, Hua Guo, James A. Quirk, James A. Dawson, and Mauro Pasta*



Cite This: *ACS Energy Lett.* 2023, 8, 2668–2673



Read Online

ACCESS |



Metrics & More

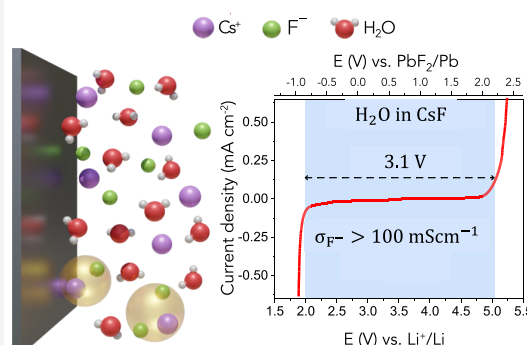


Article Recommendations



Supporting Information

ABSTRACT: The fluoride ion battery (FIB) is a promising post-lithium ion battery chemistry owing to its high theoretical energy density and the large elemental abundance of its active materials. Nevertheless, its utilization for room-temperature cycling has been impeded by the inability to find sufficiently stable and conductive electrolytes at room temperature. In this work, we report the use of solvent-in-salt electrolytes for FIBs, exploring multiple solvents to show that aqueous cesium fluoride exhibited sufficiently high solubility to achieve an enhanced (electro)chemical stability window (3.1 V) that could enable high operating voltage electrodes, in addition to a suppression of active material dissolution that allows for an improved cycling stability. The solvation structure and transport properties of the electrolyte are also investigated using spectroscopic and computational methods.



The strained supply and unforgiving costs of the critical minerals (Li, Ni, and Co) used in conventional lithium ion batteries (LIBs) have motivated an increasing interest in beyond-lithium battery chemistries.¹ Fluoride ion batteries (FIBs) utilize the fluoride shuttle between two electrodes with different (de)fluorination potentials.² The large reduction potential for the fluoride ion, attributed to its high electronegativity, promises an electrochemical stability that allows for high operating voltages, whereas the single charge and small ionic radius enable excellent transport properties with minimal polarization compared to multivalent charge carriers (e.g., Mg^{2+} , Ca^{2+} , Al^{3+}), in addition to the economic and environmental advantages allowed by the high fluoride elemental abundance.³ Furthermore, the use of conversion electrodes based on transition metal fluorides can provide theoretical energy densities of up to 1393 Wh L^{-1} (588 Wh kg^{-1}) enabled by the multielectron conversion and the high theoretical capacity of the transition metals.⁴ These merits, however, have not yet been fully realized for reversible and high energy density FIBs at room temperature (RT), with most of the previously reported FIBs using solid-state electrolytes at operating temperatures above 80°C ,^{2,5,6} and more recently at 60°C ,⁷ despite many efforts to discover and study RT fluoride conductive materials.^{8–11}

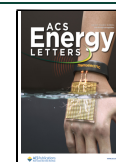
In contrast, liquid electrolytes are expected to have higher ionic conductivities that enable RT FIBs, in addition to their improved interfacial contact and compatibility with commercial LIBs manufacturing. However, their progress in FIBs has

been hindered by two factors, namely, the low solubility of the fluoride salts in the electrochemically stable aprotic organic solvents and the chemical reactivity of the fluoride ion, possibly forming the corrosive hydrofluoric acid (HF) in the presence of any acidic hydrogen.^{3,12} The two most successful liquid electrolyte designs thus far have been based on a synthesized quaternary ammonium fluoride salt dissolved in a partially fluorinated ether¹³ and cesium fluoride (CsF) solubilized in tetraglyme using boron-based anion acceptors.^{14–17} The former exhibited a 4.1 V electrochemical stability window (ESW) and a fluoride solubility of 2.1 M, but suffered from a low ionic conductivity ($<3 \text{ mS cm}^{-1}$) and significant active material dissolution that resulted in fast capacity fading of the CuF_2 cathode. On the other hand, electrolytes based on anion acceptors suffered from a similarly low ionic conductivity, a moderate ESW (ca. 2 V), and a low fluoride solubility of less than 0.5 M despite using stoichiometric amounts of the anion acceptor. Other electrolytes based on polymers¹⁸ or ionic liquids¹⁴ showed even lower conductivity or electrochemical stability.

Received: March 7, 2023

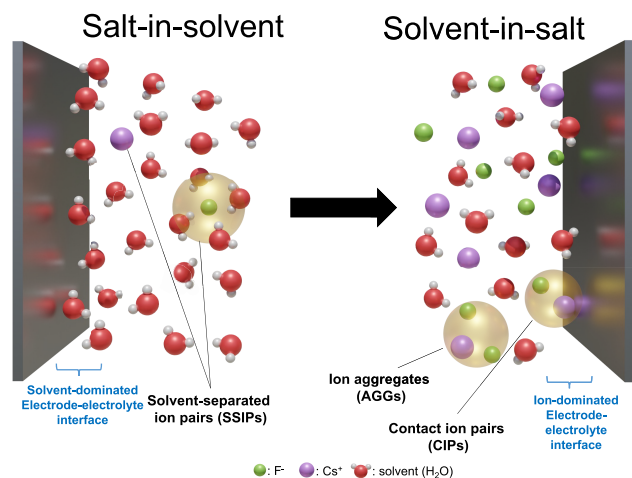
Accepted: May 15, 2023

Published: May 22, 2023



Herein, we report solvent-in-salt electrolytes for FIBs, where the low activity of the free solvent molecules results in an enhanced (electro)chemical stability and suppression of the active material dissolution, enabling more stable cycling of higher potential cathodes. At sufficiently high concentrations, the free solvent molecules and the solvent-separated ion pairs present in a traditional salt-in-solvent electrolyte evolve into contact ion pairs and ion aggregates (Scheme 1), resulting in an ion-dominated electrolyte that increases the electrochemical stability at the interface.^{19,20}

Scheme 1. Representation of the Evolution of the Ionic Species in the Bulk and the Electrode–Electrolyte Interface as the Concentration Is Increased from Salt-in-Solvent to Solvent-in-Salt Electrolytes



The solubility of CsF, a cost-effective and readily available fluoride source compared to organic-based salts, was first measured at RT in a range of protic solvents using inductively coupled plasma mass spectrometry (ICP-MS). Water was found to have by far the highest solubility of around 37 molal (*m*) (Figure 1a). Calculating the salt-to-solvent weight and volume ratios as a function of concentration showed that water was the only solvent that satisfied the theoretical solvent-in-salt condition defined by Suo et al.²¹ where both ratios exceed unity (Figure 1c). This also showed that this condition could not be satisfied for less soluble salts, such as potassium fluoride (KF), where the salt-to-solvent ratio would only exceed unity beyond the solubility limit. The high solubility of CsF in water resulted in a clear liquid electrolyte with a solvent-to-salt molar ratio of 1.7 for the saturated solution, resembling a “hydrate melt” at RT. This choice of solvent over other protic solvents was further aided by the advantageous properties of water such as the higher boiling point, inflammability, and nontoxicity, in addition to eliminating the need for ultradry cell manufacturing conditions.

Aqueous electrolytes, however, are known to have a narrow ESW, inhibiting the use of high operating voltage electrode pairs and limiting the energy density. To explore the effect of water-in-salt electrolytes (WiSEs) on expanding the ESW, linear sweep voltammetry was performed on multiple concentrations. As the concentration was increased beyond 25 *m*, the stability window was shown to expand to around 3.1 V (Figure 1d). This enhancement in the ESW is a result of the decrease in the activity of free water molecules and the

resulting change in the solvation structure, where the electrode–electrolyte interface becomes dominated by ionic species instead of the electrochemically unstable free water molecules. Very recently, a concentrated aqueous electrolyte was reported for a FIB but exhibited limited expansion in the ESW (2.1 V),²² likely due to the presence of a large fraction of free water molecules imposed by the lower solubility of KF (Figure S1).

Since solvent-in-salt electrolytes are expected to possess high viscosities that hinder ionic transport, the ionic conductivity and diffusivity were measured using electrochemical impedance spectroscopy and pulsed field gradient nuclear magnetic resonance (PFG NMR) spectroscopy, respectively. The ionic conductivity was found to peak at around 10 *m*, with the 25 *m* electrolyte exhibiting a conductivity of 152 mS cm^{−1} (Figure 2a), 2 orders of magnitude higher than for previously reported FIB organic-based electrolytes.⁴ The fluoride and cesium ion diffusivities dropped from 2.45 × 10^{−9} and 2.70 × 10^{−9} m² s^{−1}, respectively, for the 1 *m* electrolyte to 2.51 × 10^{−10} and 1.24 × 10^{−10} m² s^{−1}, respectively, for the 25 *m* electrolyte due to the increased viscosity (Figure 2b). However, the relative fluoride ion diffusion was shown to significantly improve at higher concentrations as evident by the higher transport number (Figure 2b). This improved fluoride mobility is likely attributed to a stronger O–Cs complexation in the concentrated electrolyte as the competing O–H solvent–solvent interaction is weakened due to the lower water activity.¹⁷ ¹⁷O NMR corroborated this postulate by showing the water oxygen peak at higher chemical shifts, indicating a more deshielded oxygen, in addition to a pronounced broadening indicating “solid-like” and less mobile water molecules (Figure 3a), whereas ¹H NMR showed the reverse trend (Figure S2), indicating a weakening solvent–solvent O–H bond and a strengthening O–Cs bond. This nearly immobile water network strongly complexing the cesium ion allows for a freer fluoride ion migration. Similar improved anionic migration was previously suggested in studies of lithium ion electrolytes, where the cation is known to bind more strongly to the solvent compared to the anion.²³

The solvation structure was characterized using spectroscopic and computational methods to explore the evolution from solvent–ion to ion–ion dominated interactions (Figure 3). The molecular dynamics (MD) simulation showed an increased presence of ion pairs and aggregates in the concentrated electrolyte (Figure 3c, Figure S3), in addition to a rapid decrease in the fraction of free water molecules (Figure 3b). This change in the solvation structure was reflected in the ¹⁷O NMR spectra for the water molecule, where the increased deshielding was due to a higher fraction of the water molecules donating their oxygen electrons to the Cs ions, and supported the expansion in the ESW (Figure 1d).

The chemical stability of the fluoride ion has been a major concern in FIBs, where incautious electrolyte design can result in the fluoride ion forming corrosive HF. In protic media, the fast hydrogen exchange due to the HF/F[−] equilibrium is known to result in a single ¹⁹F NMR signal with a chemical shift at the average position of all the fluoride species,²⁴ making ¹⁹F NMR inadequate in quantifying the HF content in protic solvents. Diluted aqueous fluoride electrolytes are, however, still expected to have some equilibrating HF given the pK_a value of 3.8, despite this not preventing their stable and reversible cycling for over 1000 cycles in previous reports.²⁵ The HF fraction was therefore calculated from the proton

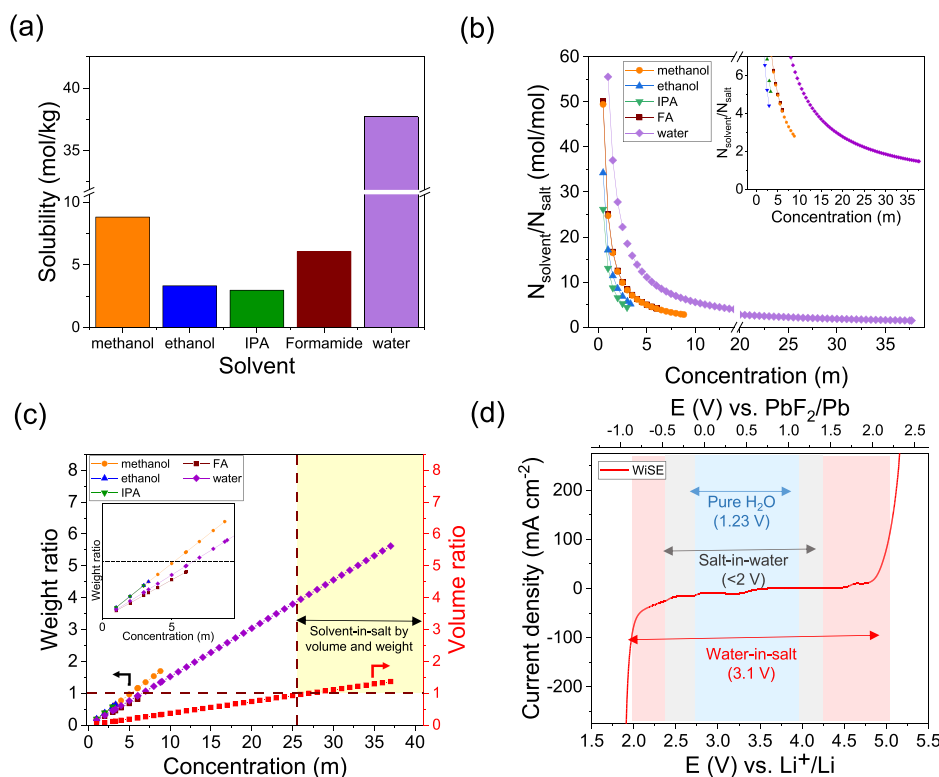


Figure 1. Solubility of CsF determined using ICP-MS in common protic solvents (a), solvent-to-salt molar ratio showing <2 coordination number for CsF in water (b), salt-to-solvent weight and volume ratios showing the concentration range of “solvent-in-salt” (c), and electrochemical stability window expansion in the water-in-salt electrolyte (this work) compared to pure water and other aqueous electrolytes (d).

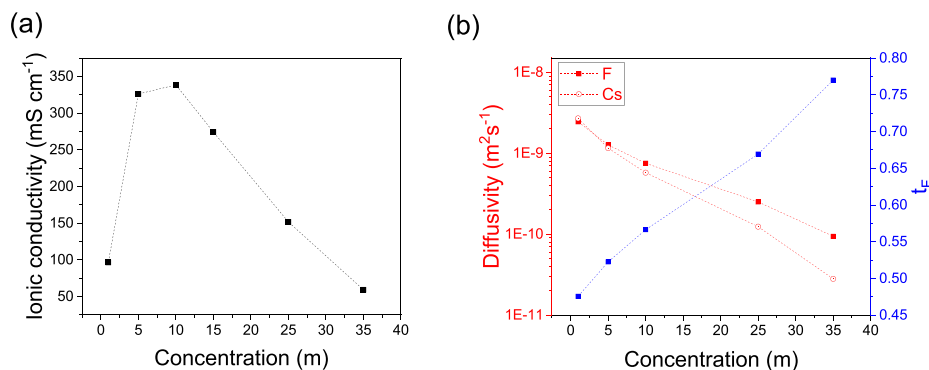


Figure 2. Ionic conductivity (a) and diffusion coefficient for the fluoride and cesium ions and the fluoride transport number (b) as a function of concentration.

activity measurement given the validity of potentiometric pH measurements at ultrahigh concentrations ($>17\text{ m}$).²⁶ The HF content was found to decrease to near zero in the WiSEs as the water molecules donating the protons became more scarce and the solution more basic (Figure 4a, Table S1). This observation is further confirmed by the increasingly deshielded fluoride in the ¹⁹F NMR (Figure 4b). Despite the difficulty of comparing the “nakedness” of the fluoride ion in multiple solvents due to other factors affecting the chemical shift (solvent electric dipole, magnetic anisotropy, etc.), comparing chemical shifts across the same solvent is a valid proxy for the fluoride solvation environment.²⁷ In this case, as the concentration is increased, the fluoride shifts away from the HF region (−160 to −170 ppm),²⁴ increasingly resembling the naked, less coordinated fluoride in organic solvents.

Furthermore, this chemical stability was accompanied by an increase in thermal stability, with a higher decomposition temperature onset and wider liquid range due to the suppressed melting point, for the WiSE (Figure S4).

Finally, to explore the RT cycling performance for the WiSE, galvanostatic cycling and CV were performed for the 25 m electrolyte, given that it exhibited an excellent trade-off between the water-in-salt properties (wide ESW and low water fraction) and transport properties (diffusion coefficient and ionic conductivity). Symmetric Pb|PbF₂ coin cells were cycled at a C/10 rate, with the low-concentration electrolyte showing faster capacity fading (Figure 5a). This is attributed to the aggravated active material dissolution at lower concentrations (given the constant solubility product, K_{sp} , lower fluoride concentrations will result in higher metal ion

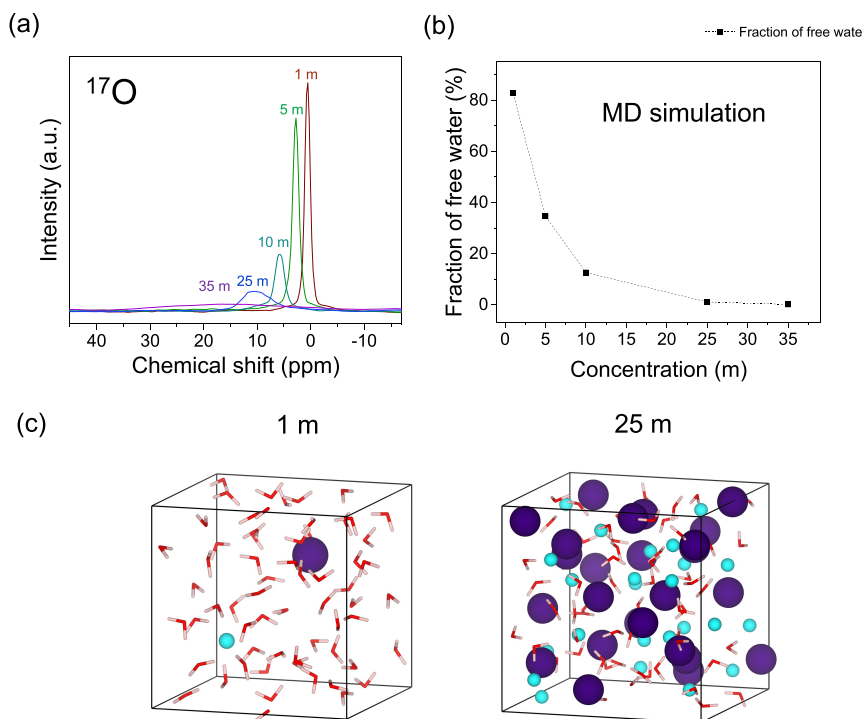


Figure 3. Solvation properties for the water-in-salt electrolyte. ^{17}O NMR spectroscopy showing the peak broadening and peak shift as the water molecules become less mobile (a), fraction of free water molecules calculated from the MD simulation (b), and MD relaxed structure at 1 and 25 m showing the formation of contact ion pairs and aggregates and elimination of free water molecules (c).

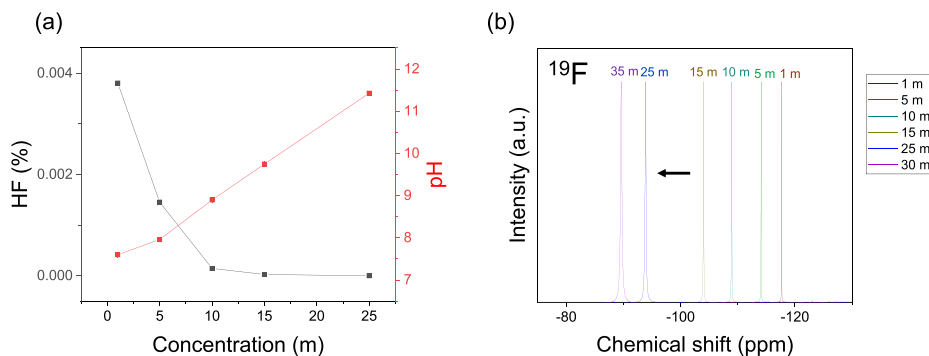


Figure 4. Fluoride ion chemical species and electronic environment. pH as a function of concentration indicating the decay of the HF content (a) and ^{19}F NMR spectroscopy (b).

dissolution), a problem known to be detrimental in previous FIBs based on conversion of metal fluorides.^{13,28,29} The WiSE, however, showed improved and more stable capacity retention, with this differentiated cycling performance expected to become more evident with further cycling.³⁰ For this symmetric cell, increased cycling showed a complete capacity loss for the diluted electrolyte by the 100th cycle (Figure S5). The cycling of the WiSE was further demonstrated for CuF_2 , where CV showed 30 cycles, compared to previous CV reports of the CuF_2 where the dissolution resulted in full capacity loss by the 10th CV cycle.¹³ The significantly suppressed CuF_2 dissolution was also visually observed as the blue color attributed to the dissolved $[\text{Cu}(\text{H}_2\text{O})]^{2+}$ being eliminated at the 25 m electrolyte (Figure S6). CuF_2 is considered to be the holy grail of cathode materials in FIBs due to its high reduction potential and high capacity (528 mAh g^{-1}),^{3,13} and a WiSE can be the system to allow for its RT stable cycling. Furthermore, the cycling of AgF_2 was shown in a fluoride shuttle system with

a potential exceeding 4 V (vs Li^+/Li), along with the cycling of ZnF_2 closer to cathodic limit of the ESW (Figure 5c). With further optimization of particle size, cathode fabrication, and careful selection of the anode materials, WiSEs have the merits to allow for further study of the fluorination mechanisms and allow for high-voltage (>2 V) FIB cycling.

In conclusion, the water-in-salt electrolyte was shown to exhibit room-temperature transport properties and (electro)-chemical stability that has been lacking in most fluoride ion battery electrolytes. NMR spectroscopy for the fluoride ion coupled with pH measurements showed a nearly complete suppression of hydrogen fluoride formation and thus an increased chemical stability. MD simulations and ^{17}O NMR shed light on the solvation structure and showed the elimination of free solvent molecules, confirming the mechanism behind the expanded electrochemical stability window. Finally, our preliminary study of the cycling performance showed an increased capacity retention for the

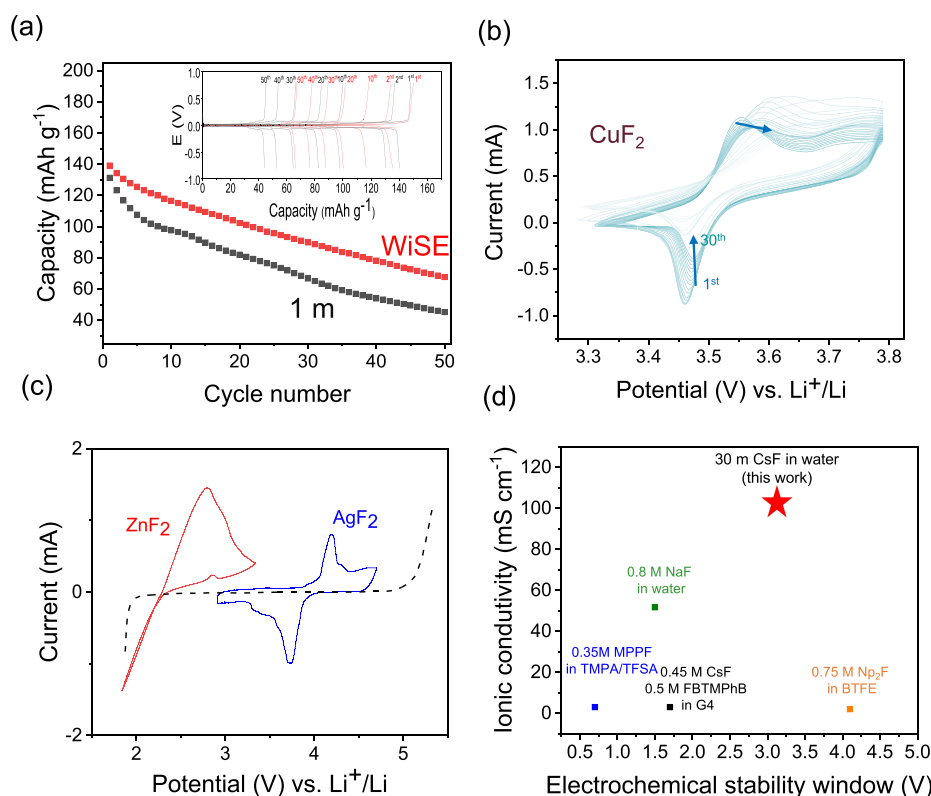


Figure 5. Galvanostatic cycling of symmetric PblPbF₂ at 1 and 25 m showing improved capacity retention in WiSE (a). Cyclic voltammetry of CuF₂ in the 25 m electrolyte (b) and of AgF₂ and ZnF₂ near the oxidative and reductive limits of WiSE (c). Performance comparison with selected fluoride ion battery electrolytes based on ESW and conductivity (d).

concentrated electrolyte, allowing for a more stable cycling and suppression of active material dissolution and offering a path for the cycling and study of the fluorination conversion mechanism for high-capacity cathode materials such as CuF₂.

■ ASSOCIATED CONTENT

Supporting Information

The Supporting Information is available free of charge at <https://pubs.acs.org/doi/10.1021/acsenergylett.3c00493>.

Materials and experimental methods for the electrochemical testing, NMR spectra, and computational calculations; supplemental figures including ¹H NMR spectra, LSV of salt-in-solvent electrolyte, Radial distribution function of MD calculation, DSC and TGA measurements, and visual characterization of the CuF₂ dissolution (PDF)

■ AUTHOR INFORMATION

Corresponding Author

Mauro Pasta – Department of Materials, University of Oxford, Oxford OX1 3PH, U.K.; orcid.org/0000-0002-2613-4555; Phone: +44 01865273777; Email: mauro.pasta@materials.ox.ac.uk

Authors

Omar Alshangiti – Department of Materials, University of Oxford, Oxford OX1 3PH, U.K.
Giulia Galatolo – Department of Materials, University of Oxford, Oxford OX1 3PH, U.K.
Gregory J. Rees – Department of Materials, University of Oxford, Oxford OX1 3PH, U.K.

Hua Guo – Department of Materials, University of Oxford, Oxford OX1 3PH, U.K.

James A. Quirk – Chemistry – School of Natural and Environmental Science, Newcastle University, Newcastle upon Tyne NE1 7RU, U.K.

James A. Dawson – Chemistry – School of Natural and Environmental Science, Newcastle University, Newcastle upon Tyne NE1 7RU, U.K.; orcid.org/0000-0002-3946-5337

Complete contact information is available at:

<https://pubs.acs.org/doi/10.1021/acsenergylett.3c00493>

Notes

The authors declare no competing financial interest.

■ ACKNOWLEDGMENTS

This work was supported by the Henry Royce Institute (through UK Engineering and Physical Science Research Council Grant EP/R010145/1) for capital equipment. O.A. thanks the Rhodes Trust and the Saudi Cultural Bureau (SACB) for funding. J.A.Q. and J.A.D. gratefully acknowledge the EPSRC (EP/V013130/1) and Newcastle University (Newcastle Academic Track (NUAcT) Fellowship) for funding via membership in the UK's HEC Materials Chemistry Consortium, which is funded by the EPSRC (EP/L000202, EP/L000202/1, EP/R029431, and EP/T022213). This work used the ARCHER2 UK National Supercomputing Service.

■ REFERENCES

(1) Choi, J. W.; Aurbach, D. Promise and reality of post-lithium-ion batteries with high energy densities. *Nat. Rev. Mater.* **2016**, *1*, 16013.

- (2) Anji Reddy, M.; Fichtner, M. Batteries based on fluoride shuttle. *J. Mater. Chem.* **2011**, *21*, 17059–17062.
- (3) Xiao, A. W.; Galatolo, G.; Pasta, M. The case for fluoride-ion batteries. *Joule* **2021**, *5*, 2823–2844.
- (4) Nowroozi, M. A.; Mohammad, I.; Molaiyan, P.; Wissel, K.; Munnangi, A. R.; Clemens, O. Fluoride ion batteries - past, present, and future. *J. Mater. Chem. A* **2021**, *9*, 5980–6012.
- (5) Rongeat, C.; Anji Reddy, M.; Witter, R.; Fichtner, M. Solid electrolytes for fluoride ion batteries: Ionic conductivity in polycrystalline tysonite-type fluorides. *ACS Appl. Mater. Interfaces* **2014**, *6*, 2103–2110.
- (6) Wissel, K.; Schoch, R.; Vogel, T.; Donzelli, M.; Matveeva, G.; Kolb, U.; Bauer, M.; Slater, P. R.; Clemens, O. Electrochemical Reduction and Oxidation of Ruddlesden-Popper-Type $\text{La}_2\text{NiO}_3\text{F}_2$ -within Fluoride-Ion Batteries. *Chem. Mater.* **2021**, *33*, 499–512.
- (7) Yu, Y.; Lei, M.; Li, D.; Li, C. Near-Room-Temperature Quasi-Solid-State F-Ion Batteries with High Conversion Reversibility Based on Layered Structured Electrolyte. *Adv. Energy Mater.* **2023**, *13*, 2203168.
- (8) Sundberg, J. D.; Druffel, D. L.; McRae, L. M.; Lanetti, M. G.; Pawlik, J. T.; Warren, S. C. High-throughput discovery of fluoride-ion conductors via a decoupled, dynamic, and iterative (DDI) framework. *npj Comput. Mater.* **2022**, *8*, 106.
- (9) Mohammad, I.; Witter, R.; Fichtner, M.; Anji Reddy, M. Room-Temperature, Rechargeable Solid-State Fluoride-Ion Batteries. *ACS Appl. Energy Mater.* **2018**, *1*, 4766–4775.
- (10) Wang, J.; Ma, C. Superior room-temperature cycling stability of fluoride-ion batteries enabled by solid electrolytes synthesized by the solid-state reaction. *Sci. China Mater.* **2022**, *65*, 3025–3032.
- (11) Kawahara, K.; Ishikawa, R.; Nakayama, K.; Shibata, N.; Ikuhara, Y. Room temperature fluoride ion conductivity in defective β - $\text{KSb1-}\delta\text{F4-3}\delta$ polycrystals. *J. Power Sources* **2021**, *483*, 229173.
- (12) Gopinadh, S. V.; Phanendra, P. V. R. L.; John, B.; Mercy, T. D. Fluoride-ion batteries: State-of-the-art and future perspectives. *Sustainable Mater. Technol.* **2022**, *32*, No. e00436.
- (13) Davis, V. K.; et al. Room-temperature cycling of metal fluoride electrodes: Liquid electrolytes for high-energy fluoride ion cells. *Science* **2018**, *362*, 1144–1148.
- (14) Okazaki, K. I.; Uchimoto, Y.; Abe, T.; Ogumi, Z. Charge-Discharge Behavior of Bismuth in a Liquid Electrolyte for Rechargeable Batteries Based on a Fluoride Shuttle. *ACS Energy Lett.* **2017**, *2*, 1460–1464.
- (15) Konishi, H.; Minato, T.; Abe, T.; Ogumi, Z. Triphenylboroxine and Triphenylborane as Anion Acceptors for Electrolyte in Fluoride Shuttle Batteries. *Chem. Lett.* **2018**, *47*, 1346–1349.
- (16) Celik Kucuk, A.; Minato, T.; Yamanaka, T.; Abe, T. Effects of LiBOB on salt solubility and BiF_3 electrode electrochemical properties in fluoride shuttle batteries. *J. Mater. Chem. A* **2019**, *7*, 8559–8567.
- (17) Celik Kucuk, A.; Abe, T. Borolan-2-yl involving anion acceptors for organic liquid electrolyte-based fluoride shuttle batteries. *J. Fluorine Chem.* **2020**, *240*, 109672.
- (18) Gschwind, F.; Bastien, J. Parametric investigation of room-temperature fluoride-ion batteries: Assessment of electrolytes, Mg-based anodes, and BiF_3 -cathodes. *J. Mater. Chem. A* **2015**, *3*, 5628–5634.
- (19) Suo, L.; Borodin, O.; Gao, T.; Olguin, M.; Ho, J.; Fan, X.; Luo, C.; Wang, C.; Xu, K. “Water-in-salt” electrolyte enables high-voltage aqueous lithium-ion chemistries. *Science* **2015**, *350*, 938–943.
- (20) Yamada, Y.; Usui, K.; Sodeyama, K.; Ko, S.; Tateyama, Y.; Yamada, A. Hydrate-melt electrolytes for high-energy-density aqueous batteries. *Nat. Energy* **2016**, *1*, 16129.
- (21) Suo, L.; Hu, Y. S.; Li, H.; Armand, M.; Chen, L. A new class of Solvent-in-Salt electrolyte for high-energy rechargeable metallic lithium batteries. *Nat. Commun.* **2013**, *4*, 1481.
- (22) Fang, Z.; Li, M.; Wang, L.; Duan, X.; Zhao, H. A long-life aqueous Fluoride-ion battery based on Water-in-salt electrolyte. *Inorg. Chem. Commun.* **2023**, *148*, 110275.
- (23) Xu, K. Electrolytes and interphases in Li-ion batteries and beyond. *Chem. Rev.* **2014**, *114*, 11503–11618.
- (24) Christe, K. O.; Wilson, W. W. Nuclear magnetic resonance spectrum of the fluoride anion. *J. Fluorine Chem.* **1990**, *46*, 339–342.
- (25) Li, X.; Tang, Y.; Zhu, J.; Lv, H.; Xu, Y.; Wang, W.; Zhi, C.; Li, H. Initiating a Room-Temperature Rechargeable Aqueous Fluoride-Ion Battery with Long Lifespan through a Rational Buffering Phase Design. *Adv. Energy Mater.* **2021**, *11*, 2003714.
- (26) Licht, S. pH Measurement in Concentrated Alkaline Solutions. *Anal. Chem.* **1985**, *57*, 514–519.
- (27) Gerken, M.; Boatz, J. A.; Kornath, A.; Haiges, R.; Schneider, S.; Schroer, T.; Christe, K. O. The ^{19}F NMR shifts are not a measure for the nakedness of the fluoride anion. *J. Fluorine Chem.* **2002**, *116*, 49–58.
- (28) Konishi, H.; Minato, T.; Abe, T.; Ogumi, Z. Charge and Discharge Reactions of a Lead Fluoride Electrode in a Liquid-Based Electrolyte for Fluoride Shuttle Batteries: The Role of Triphenylborane as an Anion Acceptor. *ChemistrySelect* **2019**, *4*, 5984–5987.
- (29) Yamanaka, T.; Abe, T.; Nishio, K.; Ogumi, Z. In Situ Observation of Fluoride Shuttle Battery Reactions with Dissolution-Deposition Mechanisms by Raman Microscopy. *J. Electrochem. Soc.* **2019**, *166*, A635–A640.
- (30) Khalid, S.; Pianta, N.; Mustarelli, P.; Ruffo, R. Use of Water-In-Salt Concentrated Liquid Electrolytes in Electrochemical Energy Storage: State of the Art and Perspectives. *Batteries* **2023**, *9*, 47.

Recommended by ACS

Nonfluorinated Antisolvents for Ultrastable Potassium-Ion Batteries

Jie Wen, Bingan Lu, et al.

AUGUST 10, 2023
ACS NANO

READ 

Mechanochemical Synthesis and Fluoride Ion Conductivity Studies in SrSnF_4 Polymorphs

Katapalli Ramakrushna Achary, Laxmi Narayana Patro, et al.

APRIL 17, 2023
THE JOURNAL OF PHYSICAL CHEMISTRY C

READ 

Understanding the Improved Fast Charging Performance of Graphite Anodes with a Fluoroethylene Carbonate Additive by In Situ NMR and EPR

Shinuo Kang, Bingwen Hu, et al.

JULY 05, 2023
ACS APPLIED ENERGY MATERIALS

READ 

Oxyfluoride Cathode for All-Solid-State Fluoride-Ion Batteries with Small Volume Change Using Three-Dimensional Diffusion Paths

Yanchang Wang, Yoshiharu Uchimoto, et al.

NOVEMBER 14, 2022
CHEMISTRY OF MATERIALS

READ 

Get More Suggestions >